Vibration Power Flow Analysis of a Gearbox Isolation System

Dongyan Shi, Xianjie Shi, and Lingcheng Kong

***Abstract*—The power flow analysis of a gearbox isolation system is carried out in accordance with the structural characteristics of a gearbox. Numerical simulation is conducted to study the influence of major structural parameters on the power flow of a gearbox isolation system. The present research can provide a theoretical basis for the vibration isolation system design of a gearbox.**

***Index Terms*—Power flow, Gearbox, Vibration isolation, Vibration characteristics**

I. Introduction

A gearbox is widely used in modern industries, because its general parts are necessary for transmitting the movement and power in mechanical equipment. The frequency of its vibration is often quite high. Double-deck isolation has a good effect on the vibration isolation of high frequency [1−3], and is considered as the main method for the vibration isolation of the gearbox of mechanical equipment. Therefore, the present research is very important in conducting vibration analysis of a structure.

The fundamental concept of power flow has been discussed by Goyder and White [4]. This is a new method used for predicting vibration energy density and the intensity of complex structures. According to the power flow theory, the transfer of vibration is primarily a transmission of energy. In recent years, this approach has been developed and applied to model complex structures and assess passive, active, and vibration control systems [5−7]. The power flow model can be used to describe the vibration propagation in structures. Thus, it is more scientific and reasonable to study vibration from the point of view of energy. The investigation of vibration transmission characteristics of the complex system from the point of view of power flow is one of the leading research issues in the field of vibration and noise control.

The vibration power flow analysis of a gearbox isolation system is carried out in the present paper. The influential factor of the vibration isolation effect is studied, which provides some theoretical reference for the isolation design of a gearbox. The vibration isolation effect also has some practical values for the application of a gearbox.

Manuscript received May 13, 2011; revised July 22, 2011. This work was funded by the International Exchange Program of Harbin Engineering University for Innovation-oriented Talents Cultivation.

Dongyan Shi is with College of Mechanical and Electrical Engineering, Harbin Engineering University, Harbin, 150001, China (phone: +86 139 3624 6286; fax: +86 451 82569288; e-mail: shidongyan@hrbeu.edu.cn).

Xianjie Shi is with College of Mechanical and Electrical Engineering, Harbin Engineering University, Harbin, 150001, China (e-mail: xianjieshi@hotmail.com)

Lingcheng Kong is with College of Mechanical and Electrical Engineering, Harbin Engineering University, Harbin, 150001, China (e-mail: konglingcheng@hrbeu.edu.cn)

II. Isolation Scheme Of a Gearbox

Depending on the type of equipment, weight of the middle mass and structure size, the isolation system of a gearbox is designed based on specific isolation design specifications [8]. The double-deck isolation system of a gearbox consists of: (1) rigid mass representing a gearbox; (2) isolators; and (3) an elastic base plate (as shown in Fig. 1). The layout of the isolators is shown in Fig. 2.

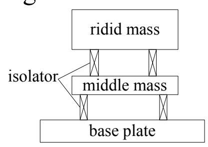

Fig. 1. Gearbox isolation system

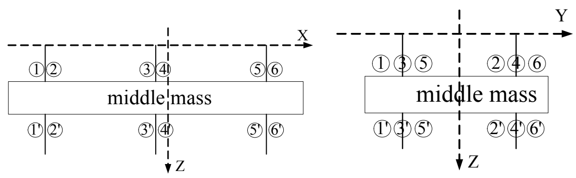

Fig. 2. Layout of the isolators

III. Power Flow Transmission Of the Double-Deck Isolation System

A. *Transfer Matrix*

Fig. 3 shows that the double-deck isolation system of a gearbox can be expressed. There are five substructures in this system. The power flow transmission of the isolation system can be solved using a solution consisting of substructure mobility matrixes.

To solve the transfer matrix of the double-deck isolation system, it should be divided into two subsystems that are equivalent to the superposition of the two single vibration isolation systems, respectively. The subsystems are shown in Fig. 4.

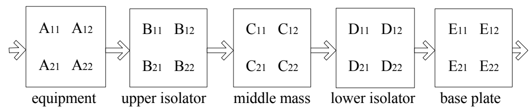

Fig. 3. The energy transmission of double-deck isolation system

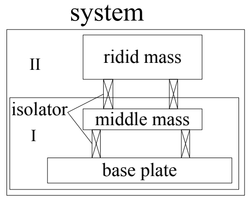

Fig. 4. The subsystem of the double-deck isolation system

ISBN: 978-988-19251-7-6
ISSN: 2078-0958 (Print); ISSN: 2078-0966 (Online)

The four-pole parameters method is a classical technique for deriving the dynamic characteristics of an assembled system that are connected in series or in parallel. This method is considered practical for a single-input/single-output linear vibration system [9].

The response relationship between force and velocity for the equipment can be expressed as:

$$\begin{bmatrix} V_I \\ V_A \end{bmatrix} = \begin{bmatrix} A_{11} & A_{12} \\ A_{21} & A_{22} \end{bmatrix} \begin{bmatrix} F_I \\ F_A \end{bmatrix} . \tag{1}$$

We arrive at the following according to the four-pole parameters relationship of the upper isolators:

$$\begin{bmatrix} F_A \\ V_A \end{bmatrix} = \begin{bmatrix} B_{11} & B_{12} \\ B_{21} & B_{22} \end{bmatrix} \begin{bmatrix} F_B \\ V_B \end{bmatrix} . \tag{2}$$

The response relationship between the force and velocity for middle mass can be expressed as:

$$\begin{bmatrix} V_B \\ V_C \end{bmatrix} = \begin{bmatrix} C_{11} & C_{12} \\ C_{21} & C_{22} \end{bmatrix} \begin{bmatrix} F_B \\ F_C \end{bmatrix} . \tag{3}$$

We arrive at the following according to the four-pole parameters relationship of the lower isolator:

$$\begin{bmatrix} F_C \\ V_C \end{bmatrix} = \begin{bmatrix} D_{11} & D_{12} \\ D_{21} & D_{22} \end{bmatrix} \begin{bmatrix} F_D \\ V_D \end{bmatrix} . \tag{4}$$

The relationship between force and velocity for the elastic base can be expressed as:

$$V_D = M_E F_D \ , \tag{5}$$

where $[A]$, $[C]$, and $[M_E]$ are the mobility matrices of the equipment, middle mass and elastic base, respectively; and $[B]$ and $[D]$ are the transfer matrices of the upper and lower isolators, respectively.

The subsystem transfer matrix $[T_I]$ can be expressed as:

$$T_I = \left[D_{21} + D_{22} M_E - C_{22} \left(D_{11} + D_{12} M_E \right) \right]^{-1} C_{21} . \tag{6}$$

From formula (4), $[F_C]$ can be expressed as:

$$F_C = D_{11} F_D + D_{12} V_D . \tag{7}$$

From formula (3), V_B can be expressed as:

$$V_B = C_{11} F_B + C_{12} F_C . \tag{8}$$

Formulas (5) and (7) are substituted into Formula (8); thus, $[V_B]$ can be expressed as:

$$V_B = \left[C_{11} + C_{12} (D_{11} + D_{12} M_E) T_{I1} \right] F_B . \tag{9}$$

Suppose $G = C_{11} + C_{12}(D_{11} + D_{12} M_E) T_{I1}$; thus, V_B can be described as:

$$V_B = [G] F_B \ . \tag{10}$$

where $[G]$ is the mobility matrix of subsystem I.

The transfer matrix of subsystem II can be solved with the same method. Its expression is given by:

$$T_{II} = [B_{21} + B_{22} G - A_{22} \left(B_{11} + B_{12} G \right)]^{-1} A_{21} . \tag{11}$$

Therefore, the total transfer matrix of the double-deck isolation system can be expressed as:

$$\begin{aligned} T &= T_I T_{II} \\ &= \left\{ \left[D_{21} + D_{22} M_E - C_{22} \left(D_{11} + D_{12} M_E \right) \right]^{-1} C_{21} \right\} \cdot \\ &\quad \cdot \left\{ [B_{21} + B_{22} G - A_{22} \left(B_{11} + B_{12} G \right)]^{-1} A_{21} \right\} \end{aligned} \tag{12}$$

B. The Power Flow of the Isolation System

In the condition of force $F(t)$ and velocity $V(t)$, the input average power is the vibration power flow. This can be calculated using Formula (13) given by:

$$P = \frac{1}{T} \int_0^T (F \cdot V) dt . \tag{13}$$

Vibration power flow can comprehensively reflect the energy intensity, which is transmitted into the structure from external excitation. For a harmonic excitation and response, the excitation and velocity response can be expressed as: $F = |F| e^{i\omega t}$ and $V = |V| e^{i(\omega t + \varphi)}$. Therefore, the vibration power flow can be described as:

$$\begin{aligned} P &= \frac{1}{T} \int_0^T (F \cdot V) dt = \frac{\omega}{2\pi} \int_0^{\frac{2\pi}{\omega}} \mathrm{Re}(F) \mathrm{Re}(V) dt \\ &= \frac{1}{2} |F| \cdot |V| \cos\varphi = \frac{1}{2} \mathrm{Re}(F^H \cdot V) \end{aligned} . \tag{14}$$

Thus, the power flow transmitted into the system can be expressed as:

$$\begin{aligned} P_I &= \frac{1}{2} \mathrm{Re} \left\{ (F_I)^H V_I \right\} \\ &= \frac{1}{2} \mathrm{Re} \left\{ (F_I)^H [A_{11} + A_{12} (B_{11} + B_{12} G) T_{II}] F_I \right\} \end{aligned} . \tag{15}$$

With the same method, the power flow transmitted into the middle mass and elastic base can be calculated with Formulas (16) and (17) respectively given as:

$$\begin{aligned} P_C &= \frac{1}{2} \mathrm{Re} \left\{ (F_C)^H V_C \right\} \\ &= \frac{1}{2} \mathrm{Re} \left\{ F_I^{\,H} T^H (D_{11}^{\,H} + M_E^{\,H} D_{12}^{\,H})(D_{21} + D_{22} M_E) T F_I \right\} \end{aligned} \tag{16}$$

$$P_M = \frac{1}{2} \mathrm{Re} \left\{ (F_D)^H V_D \right\} = \frac{1}{2} \mathrm{Re} \left\{ F_I^{\,H} T^H M_E T F_I \right\} . \tag{17}$$

IV. Mobility Matrix Of the Subsystem Structure

A. Mobility Matrix of the Equipment

The equipment is treated as a rigid body that has six degrees of freedom. The contact between the isolator and equipment is called the point contact. The force state of the rigid body is analyzed with the knowledge of rigid body dynamics. The force diagram of the equipment is shown in Fig. 5. In consideration of the general problems, the number of isolators is *s*, where $s = 1, 2, 3 \cdots$.

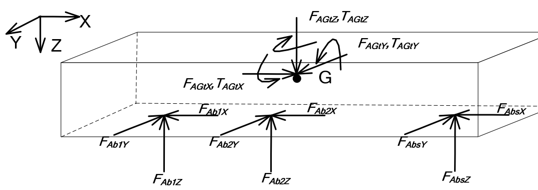

Fig. 5. The force diagram of the equipment

The force and velocity response of the equipment centroid

ISBN: 978-988-19251-7-6
ISSN: 2078-0958 (Print); ISSN: 2078-0966 (Online)

is respectively shown as follows:

$$F_{AGt} = \begin{bmatrix} F_{AGtX} & F_{AGtY} & F_{AGtZ} & T_{AGtX} & T_{AGtY} & T_{AGtZ} \end{bmatrix}^T \tag{18}$$

$$V_{AGt} = \begin{bmatrix} V_{AGtX} & V_{AGtY} & V_{AGtZ} & \dot{\theta}_{AGtX} & \dot{\theta}_{AGtY} & \dot{\theta}_{AGtZ} \end{bmatrix}^T . \tag{19}$$

The force and velocity response of the contact point is given by F_{Ab} and V_{Ab}, respectively. They are transformed into equipment centroid G, which can be respectively described as:

$$F_{AGb} = \begin{bmatrix} F_{AGbX} & F_{AGbY} & F_{AGbZ} & T_{AGbX} & T_{AGbY} & T_{AGbZ} \end{bmatrix}^T \tag{20}$$

$$V_{AGb} = \begin{bmatrix} V_{AGbX} & V_{AGbY} & V_{AGbZ} & \dot{\theta}_{AGbX} & \dot{\theta}_{AGbY} & \dot{\theta}_{AGbZ} \end{bmatrix}^T . \tag{21}$$

The relationship between force, velocity response, and transformed force and velocity can be written as:

$$F_{AGb} = T_{AFb} F_{Ab} , \tag{22}$$

$$V_{Ab} = T_{AVb} V_{AGb} . \tag{23}$$

According to the dynamic equilibrium equations, the following equation can be obtained by:

$$\left[F_{AGt}\right]_{6\times1} + \left[F_{AGb}\right]_{6\times1} = \left[W\right]_{6\times6} \left[V_{AGt}\right]_{6\times1} . \tag{24}$$

In consideration of these equations, the relationship between force and velocity can be obtained by:

$$\begin{bmatrix} V_{AGt} \\ V_{Ab} \end{bmatrix} = \begin{bmatrix} W^{-1} & W^{-1}T_{AFb} \\ T_{AVb}W^{-1} & T_{AVb}W^{-1}T_{AFb} \end{bmatrix} \begin{bmatrix} F_{AGt} \\ F_{Ab} \end{bmatrix} . \tag{25}$$

Therefore, the mobility matrix of the equipment is given by:

$$A = \begin{bmatrix} W^{-1} & W^{-1}T_{AFb} \\ T_{AVb}W^{-1} & T_{AVb}W^{-1}T_{AFb} \end{bmatrix} . \tag{26}$$

B. The Mobility Matrix of the Middle Mass

The force diagram of the middle mass is shown in Fig. 6. The number of the upper isolator is *s*, where $s = 1, 2, 3 \cdots$, and the number of the lower isolator is *n*, where $n = 1, 2, 3 \cdots$.

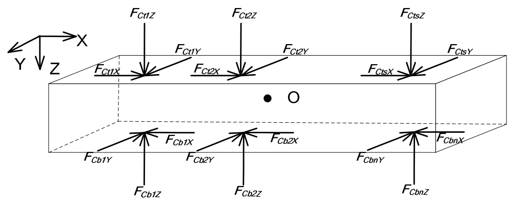

Fig. 6. The force diagram of the middle mass

According to the calculation of the equipment, the formula can be obtained using the dynamic equilibrium equation given by:

$$\left[F_{COt}\right]_{6\times1} + \left[F_{COb}\right]_{6\times1} = \left[W\right]_{6\times6} \left[V_{COt}\right]_{6\times1} . \tag{27}$$

The relationship between these forces and velocities are shown as follows:

$$F_{COt} = T_{CFt} F_{Ct} , \tag{28}$$

$$V_{Ct} = T_{CVt} V_{COt} , \tag{29}$$

$$F_{COb} = T_{CFb} F_{Cb} , \tag{30}$$

$$V_{Cb} = T_{CVb} V_{COb} . \tag{31}$$

The relationship between the velocity and force can be written as follows:

$$\begin{bmatrix} V_{Ct} \\ V_{Cb} \end{bmatrix} = \begin{bmatrix} T_{CVt}W^{-1}T_{CFt} & T_{CVt}W^{-1}T_{CFb} \\ T_{CVb}W^{-1}T_{CFt} & T_{CVb}W^{-1}T_{CFb} \end{bmatrix} \begin{bmatrix} F_{Ct} \\ F_{Cb} \end{bmatrix} \tag{32}$$

Therefore, the mobility matrix of the middle mass is given by:

$$C = \begin{bmatrix} T_{CVt}W^{-1}T_{CFt} & T_{CVt}W^{-1}T_{CFb} \\ T_{CVb}W^{-1}T_{CFt} & T_{CVb}W^{-1}T_{CFb} \end{bmatrix} . \tag{33}$$

C. The Mobility Matrix of the Upper and Lower Isolator

The force diagram of the isolator is shown in Fig. 7. In the analysis, the mass of the isolator is ignored, which is then treated as the spring-damper system.

Under harmonic excitation, the displacement and velocity response can be described in the following forms:

$$x = Xe^{j\omega t} , \tag{34}$$

$$\dot{x} = j\omega x . \tag{35}$$

According to Hooke's law, the force can be described as:

$$F = k\frac{\dot{x}}{j\omega} . \tag{36}$$

For the isolator of Fig. 7, we use:

$$F_{ti} = F_{bi} , \tag{37}$$

$$F_{ti} = \frac{k}{j\omega}\left(V_{bi} - V_{ti}\right) . \tag{38}$$

Thus, we obtain the four-pole parameters transfer matrix equation of the isolator given by:

$$\begin{bmatrix} F_t \\ V_t \end{bmatrix} = \begin{bmatrix} B_{11} & B_{12} \\ B_{21} & B_{22} \end{bmatrix} \begin{bmatrix} F_b \\ V_b \end{bmatrix} . \tag{39}$$

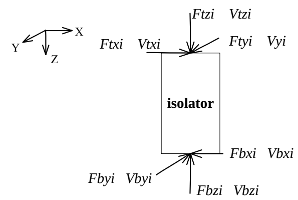

Fig. 7. The force diagram of the isolator

D. Mobility Matrix of the Elastic Base

The mobility matrix of the elastic base is analyzed systematically. The solution formula of the mobility matrix of a simply supported plate is shown as follows [10]:

$$M_{j,k} = \frac{4i\omega}{\rho hab}\sum_{m=1}^{\infty}\sum_{n=1}^{\infty}\frac{\varphi_{mn}(h_j, b/2)\cdot\varphi_{mn}(h_k, b/2)}{\omega_{mn}^2(1+i\delta)-\omega^2} , \tag{40}$$

where $i, k = 1, 2, \cdots, \mathrm{N}$; and

ρ, δ, h, a, b are the density, damping ratio, thickness, length and width of the elastic base, respectively;

h_j, h_k are the positions of the isolators in the elastic base; and

$\varphi_{mn}, \omega_{mn}$ are the mode-shaped functions and vibration frequency of the rectangular plate without damping.

V. Numerical Simulation and Discussion

The results of the computer simulations for the power flow of a gearbox isolation system are presented in this section. The isolation system parameters are given in Table 1. First, to evaluate the power flow of the isolation system, three power flow curves were obtained from this model, including the power flow transmitted into the equipment, middle mass, and base (Fig. 8).

Fig. 8 indicates that the power flow transmitted into the equipment, middle mass, and base decreases with the increase of excitation frequency, especially in the high

ISBN: 978-988-19251-7-6
ISSN: 2078-0958 (Print); ISSN: 2078-0966 (Online)

frequency. Therefore, double-deck isolation system has better isolation effect on the equipment with high excitation frequency.

Let us use this model to study the effect of the elastic base damping ratio and stiffness on the power flow.

The effect result under different elastic modulus of the base plate is shown in Fig. 9. For a structure, its stiffness can be increased with an increase of the elastic modulus. Consequently, the natural frequency of the structure can increase as well. Fig. 9 indicates that the resonance peak in high frequency of a corresponding power flow curve moves to a high frequency with the increase of a base plate elasticity modulus. This is ideal for vibration isolation. In addition, Fig. 9 also explains that the resonance peak in high frequency is excited by the natural frequency of the base plate.

Fig. 10 indicates that the damping of the base plate has a great influence on the power flow transmission of the isolation system. The energy transmitted into the base plate is reduced greatly by reducing the damping ratio of the base plate. However, increasing the damping ratio of the base plate has a positive effect on the weakening high frequency resonance peak, which is excited by the natural frequency of the base plate. Some high order mode can be inhibited with the increase of the damping ratio. Therefore, the resulting isolation effect is poor with a small damping ratio.

TABLE I
STRUCTURE PARAMETERS OF A GEARBOX DOUBLE-DECK ISOLATION SYSTEM

Item	Value	Item		Value
Damping ratio of isolator	0.15	Length of base plate	mm	1600
Damping ratio of base plate	0.02	Width of base plate		700
Young modulus of base plate MPa	2.1E5	Length of middle mass		1000
Density of base plate kg/mm^3	7.8E-6	Width of middle mass		460

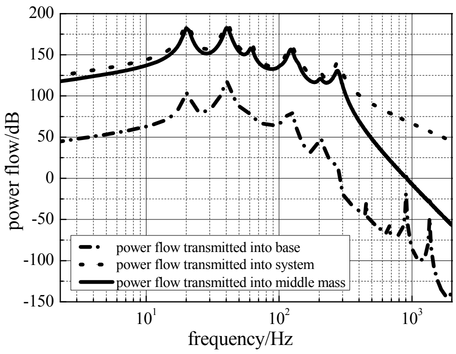

Fig. 8. The power flow of the equipment, middle mass, and elastic base

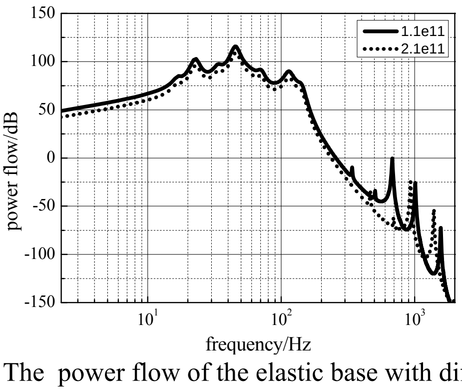

Fig. 9. The power flow of the elastic base with different Young's modulus values

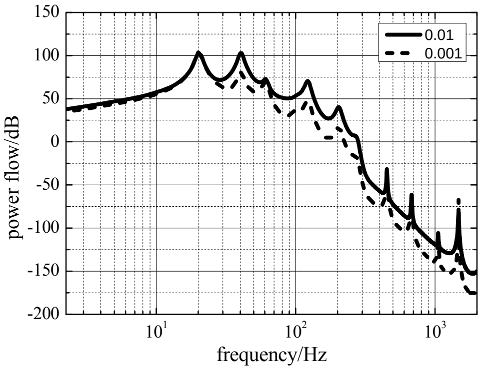

Fig. 10. The power flow of the elastic base with different damping ratios

VI. CONCLUSIONS

The mobility matrices of each subsystem for a double-deck isolation system are derived using the admittance theory. Under the condition of complex excitation, power-flow transfer characteristic of multi-freedom, the double-deck isolation system is studied using the power flow theory. The formulas of power flow transmission with elastic base are created with an analysis of the double-deck isolation system. The power flow, which is obtained with numerical simulation, is then transmitted into the base, middle mass and base plate. Power flow decreases with the increase of excitation frequency, especially in the high frequency. Thus, the double-deck isolation system is ideal for high frequency isolation. Finally, the effects of the elastic base damping ratio and stiffness on the power flow are studied. According to the results, in order to achieve the best isolation performance, the base plate parameters effect should be considered during the system design. In-depth studies must also be carried out in the future to study this effect further.

REFERENCES

[1] Ungar E and Dietrich C W, "High-frequency vibration isolation," Journal of Sound and Vibration, vol. 4, no. 2, pp. 224-241, 1966.
[2] Zhang Weibo, Liu Hui, Li Fanbing and Song Xianchun, "Power Flow transmission Characteristics of the Structure Sound in Gearbox-like System," China Mechanical Engineering, vol. 19, no. 14, pp. 1724-1726, 2008.
[3] W.J. Choi, Y.P. Xiong and R.A. Shenoi, "Power flow analysis for a floating sandwich raft isolation system using a higher-order theory," Journal of Sound and Vibration, vol. 319, no. 1-2, pp. 228-246, 2009.
[4] H.G.D. Goyder and R.G. White, "Vibration power flow from machines into built-up structures," Journal of Sound and Vibration, vol. 68, pp. 59-117, 1980.
[5] Y.P. Xiong and K.J. Song, "Power flow analysis for a new isolation system-flexible floating raft," Chinese Journal of Mechanical Engineering, vol.9, no. 3, pp. 260-264, 1996.
[6] J. Pan, J. Pan and C.H. Hansen, "Total power flow from a vibrating rigid body to a thin panel through multiple elastic mounts", The Journal of the Acoustical Society of America, vol. 92, no. 2, pp. 895-907, 1992.
[7] Chun-Chuan Liu, Feng-Ming Li and Bo Fang, "Active control of power flow transmission in finite connected plate," Journal of Sound and Vibration, vol.329, no. 20, pp. 4124-4135, 2010.
[8] F.F. Yap, N. Vahdati and H. Harmoko, "Design and analysis of vibration isolation systems for hard disk drives", Journal of Magnetism and Magnetic Materials, vol. 303, no. 2, pp. 59-56, 2006.
[9] Shi-jian Zhu and Lin He, Vibration control of onboard machinery, National defense industry press, 2006.
[10] P.Gardonio, S. J. Elliott and R. J. Pinnington, "Active isolation of structural vibration on multiple-degree of freedom system, Part I: The dynamics of the system", Journal of Sound and Vibration, vol. 207, no. 1, pp. 61-93, 1997.